CSCE 2021 Annual Conference
Inspired by Nature – Inspiré par la Nature

26-29 May 2021

RELIABILITY-BASED EVALUATION OF THE STIFFNESS REDUCTION FACTOR FOR SLENDER GFRP REINFORCED CONCRETE COLUMNS

Khorramian, Koosha[1,4], Oudah, Fadi[2], and Sadeghian, Pedram[3]
[1] Postdoctoral Fellow, Department of Civil and Resource Engineering, Dalhousie University
[2] Assistant Professor, Department of Civil and Resource Engineering, Dalhousie University
[3] Associate Professor and Canada Research Chair in Sustainable Infrastructure, Department of Civil and Resource Engineering, Dalhousie University
[4] Koosha.Khorramian@dal.ca

Abstract: The stiffness of concrete columns is adjusted by a factor referred to as the stiffness reduction factor or the stability resistance factor when utilizing the simplified second-order moment magnification method for designing slender reinforced concrete (RC) columns. The stiffness reduction factor of 0.75 in ACI 318, CSA A23.3, and CSA S6 was calibrated for steel-RC columns using reliability analysis to account for the variability in concrete strength, steel strength, and applied loads. The upcoming ACI 440 code adopts the same stiffness reduction factor for the design of slender glass fiber-reinforced polymer (GFRP) RC columns when using the moment magnification method. The structural reliability of slender GFRP-RC columns designed using a stiffness reduction factor of 0.75 was not evaluated despite the difference in the GFRP statistical parameters and stiffness characteristics as compared with conventional steel. The objective of this research is to conduct a reliability analysis of slender GFRP-RC columns to evaluate the reliability index associated with the use of the stiffness reduction factor and provide recommendations regarding the optimum value of the factor to meet code target safety limits. Monte Carlo simulation is used to conduct the reliability analysis. Statistical input parameters (distribution type, bias ratio, and coefficient of variation) of GFRP based on an extensive experimental database are utilized in the study. The proposed research presents a necessary step toward quantifying the safety associated with the design provisions proposed in upcoming ACI 440 code.

1 INTRODUCTION

The moment magnification method is a simplified analysis method used for the design and analysis of slender steel-reinforced concrete columns as specified in concrete design standards/codes such as ACI 318-19 (2019) and CSA A23.3-19 (2019). The moment magnification method involves the use of a stiffness reduction factor, also named as stability reduction factor, used to adjust the critical buckling strength of slender columns.

The stiffness reduction factor is a reliability-based resistance factor calibrated by Mirza et al. (1987) for ACI 318-83 (1983) and was later adopted by ACI 318-19 (2019). Mirza et al. (1987) performed a reliability analysis in which a single curvature 305 by 305 mm steel-reinforced concrete section with concrete strength of 34.5 MPa and steel yield strength of 414 MPa was used to conduct a parametric study regarding key influential design parameter. The parameters considered in the study by Mirza et al. (1987) included: reinforcement ratio, slenderness ratio, tributary areas, eccentricity ratio, and the effect of combined dead, live, snow, and wind loads. The analysis was based on the moment magnification method and second-order analysis method. A Monte Carlo simulation with 1000 trials was used to obtain the distribution of the resistance presented as the ratio of the second-order resistance to the factored capacity determined by the moment magnification method. First order second moment (FOSM) reliability method was then used to assess the reliability corresponding to each considered case. The study recommended the use of a stiffness reduction factor between 0.7 to 0.75. A value of 0.75 was adopted by ACI 318-83 (1983) and ACI 318-19 (2019).

ACI 440 committee is preparing a code for the design of glass fiber-reinforced polymer (GFRP) reinforced concrete (RC) columns in which the moment magnification method, including the stiffness reduction factors, is adopted from ACI 318-19. The stiffness reduction factor proposed in the upcoming ACI 440 code has not been validated for GFRP-RC columns. The difference between the statistical properties of GFRP and steel bars, the lack of yielding in GFRP, and the difference in the modes of failure necessitate an independent reliability-based study for GFRP-RC columns. In this research, a preliminary reliability analysis is conducted to examine the safety of slender GFRP-RC columns designed with the proposed stiffness reduction factor in ACI 440.

2 METHODOLOGY

The methodology adopted in this research is similar to Mirza et al. (1987) but with utilizing statistical parameters of GFRP bars, considering concrete crushing as the only failure mode, and considering dead and live loads only. The methodology was utilized to determine the reliability indexes, β, corresponding to multiple stiffness reduction factors, ϕ_s.

The moment magnification method is presented followed by the finite difference method of analysis. The latter was augmented with an artificial neural network to account for the second-order effects. The methods were utilized to conduct the reliability analysis.

2.1 Moment Magnification Method

The moment magnification method is a simplified analysis method used for calculating the capacity of columns considering secondary moment effects through a magnification factor, δ. The magnification factor is applied to the maximum end moment, M_2, to provide an equivalent magnified moment, M_c.

[1] $M_c = \delta M_2$

The magnification factor is calculated using Eq. 2, where C_m accounts for end moment effects (equal 1 for single curvature), P_u is the factored load, P_c is the critical buckling load, and ϕ_s is the stability reduction factor.

[2] $\delta = \frac{C_m}{1-\frac{P_u}{\emptyset_S P_c}}$

The critical buckling load, P_c, is calculated using Eq. 3, where k is the effective length of the column (equal 1 for simply supported columns), l_u is the length of the column, and EI_{eff} is the effective stiffness (ACI 318-19 2019).

[3] $P_c = \frac{\pi^2 EI_{eff}}{(kl_u)^2}$

The effective stiffness, EI_{eff}, is calculated using Eq. 4 as proposed by Zadeh and Nanni (2017) and adopted by the upcoming ACI 440 code, where E_c is the modulus of elasticity of concrete, E_f is the modulus of elasticity of GFRP bars, I_g and I_f are the moment of inertia of the gross cross-section and GFRP bars, respectively.

[4] $EI_{eff} = 0.2E_cI_g + 0.75E_fI_f$

The factored load, P_u, is calculated by setting the utilization ratio (ratio of factored load to factored resistance) equal to unity, as included in Eq. 5.

[5] $\phi_nP_n = P_u$

where, ϕ_n is the resistance reduction factor applied to the axial and flexural capacities of the column, and P_n is the nominal capacity of the column cross-section per upcoming ACI 440 code. P_n is evaluated at the ultimate compressive strain of 0.003 mm/mm.

The value of ϕ_n is considered as 0.65 in this study since experimental research indicates that the compressive failure of concrete is the only observed mode of failure (Hadhood et al., 2018, Khorramian and Sadeghian 2017a, 2017b, 2020). To find the axial factored capacity of the column using the moment magnification method, the factored load moment interaction diagram is developed, while the intersection of the loading path derived from the moment magnification method and the interaction diagram is considered as the factored axial capacity as shown in Figure 1.

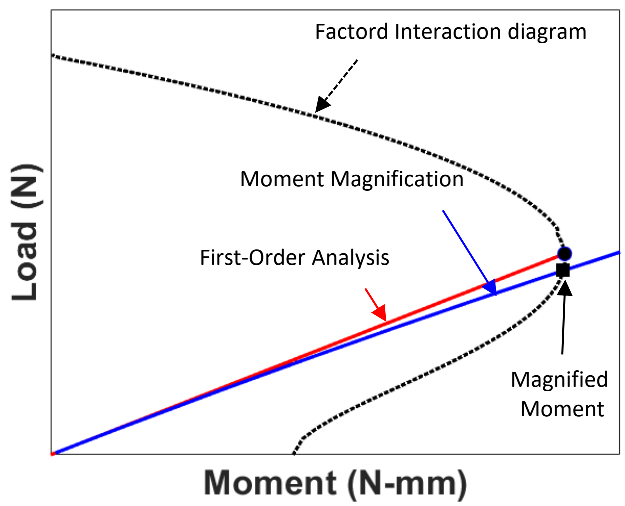

Figure 1: Illustration of the moment magnification procedure

2.2 Second-Order Analysis

The second-order analysis performed in this study is based on an artificial neural network (ANN) model. The model considered material and geometric nonlinearities. The ANN model is a surrogate model to the finite difference method (FDM) with a coefficient of determination of 1.0 and an RMSE of 1.0 kN (Khorramian et al. 2021). The column is divided into a finite number of segments in FDM, while equilibrium is satisfied at each node. An iterative procedure is used at each load step to determine the deflected shape of the column using moment-curvature. The column capacity is determined once material or stability failure occurs. Figure 2(a) presents a summary of the FDM analysis. More details about the FDM used in this study can be found in the literature (Khorramian 2020).

The schematic ANN model by Khorramian et al. (2021) is presented in Figure 2(b). The ANN model consists of one input layer with 11 neurons, 1 output layer corresponding to the axial capacity of the column, and three hidden layers with 35, 30, and 15 neurons in the first, second, and third hidden layers of ANN. A sigmoid function was used as the activation function for the hidden layers and a linear function was used for the output layer. Further information is available in the literature (Khorramian et al. 2021).

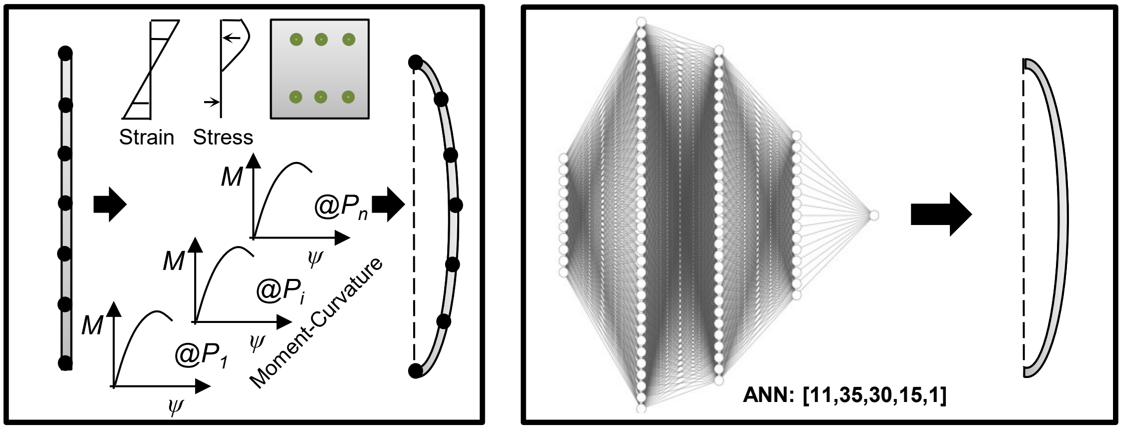

(a) (b)

Figure 2: Second-Order Analysis: (a) finite difference method (FDM); and (b) artificial neural network (ANN) method

2.3 Reliability Analysis

The reliability analysis utilized in this study is based on the procedure used to assess the safety of steel-reinforced concrete columns by Mirza et al. (1987), with the following two modification: statistical properties of GFRP were used in this study, and only concrete compression failure mode was considered in this study.

The statistical properties of the input random variables include bias (ratio of actual to predicted), coefficient of variation (COV), and distribution type. The bias, COV, and distribution type for FDM-to-experimental test results were 1.1, 0.14, normal, respectively. The bias, COV, and distribution type for dead load were 1.05, 0.15, and normal, respectively. The bias, COV, and distribution type for live load were 1.0, 0.18. and normal respectively. For concrete compressive strength, f_c, a normal distribution with a coefficient of variation of 0.1 and a bias calculated from Eq. 7, was considered (Nowak and Szerszen 2003).

[7] $k_{fc} = -0.0081f_c^3 + 0.1509f_c^2 - 0.9338f_c + 3.0649, (f_c \text{ is in } ksi)$

The depth of bars in the ultimate compressive and tensile reinforcement layers was considered to have a normal distribution with a bias of 1 and COV of 0.11 (Khorramian 2020). For GFRP bars in tension, a bias of 1.15 and COV of 0.07 with a lognormal distribution was considered (Shield et al. 2011). For the modulus of elasticity of GFRP bars, a lognormal distribution with a mean of 1.04 and COV of 0.08 was considered (Shield et al. 2011). To find the distribution and statistical characteristics of GFRP bars in compression, twelve different groups of GFRP bar tested in compression were collected from the literature, including 72 compression tests of GFRP bars by AlAjarmeh et al. (2019) and 35 compression tests of GFRP bars by Khorramian and Sadeghian (2018, 2019). Test data was normalized to the average compressive strength of each test group to form a database of 107 compressive tests of GFRP bars. Figure 3 shows the distribution of the relative compressive strength of GFRP bars. The distribution is considered as lognormal with a bias of 1 and COV of 0.13.

The first step in the reliability calculation is to determine the mean values of dead, *D*, and live, *L*, loads. The moment magnification method is used to calculate the factored resistance, which is set equal to the factored loads. Then, for a given dead-to-live load ratio, the nominal values of the *D* and *L* loads are calculated using the load combination including D and L for the upcoming ACI 440 code presented in Eq. 8, which is adapted from ACI 318-19 (2019). The nominal values were multiplied by load bias to obtain the mean value of dead and live loads.

[8] $U = 1.2D + 1.6L$

Monte Carlo simulation (MCS) with 1000 trials was utilized to find the resistance distribution. The nominal section and material properties were multiplied by their corresponding bias to obtain the mean values. One thousand randomly generated distinct input sets were provided for the ANN model to determine the corresponding resistance. Each distinct input set includes randomly generated concrete strength, reinforcement depth, strength of GFRP bars in compression and tension, reinforcement ratio of GFRP bars, modulus of elasticity of GFRP bars, eccentricity ratio, and slenderness ratio. The ratio of the ANN model-to-experimental test data was applied to the resistance. The distribution of the resistance, *R*, minus the distribution of *D* and *L* loads defines the performance function, *G*, as presented in Eq. 9.

[9] $G(X) = R(X) - L - D$

Failure occurs when the resistance is less than the sum of load effects or when the performance function is negative. To calculate the reliability index, a first-order second moment (FOSM) analysis was performed using three random variables (i.e., *R*, *D*, and *L*). The value of the reliability index can be found using Eq. 10 (Nowak and Collins 2012).

[10] $\beta = \frac{G(\mu_{X1},\mu_{X2},\ldots,\mu_{Xn})}{\sqrt{\Sigma_{i=1}^{n}(a_i\sigma_{Xi})^2}}$, $a_i = \frac{\partial G}{\partial Xi}\Big|_{@\ \mu_{X1},\mu_{X2},\ldots,\mu_{Xn}}$

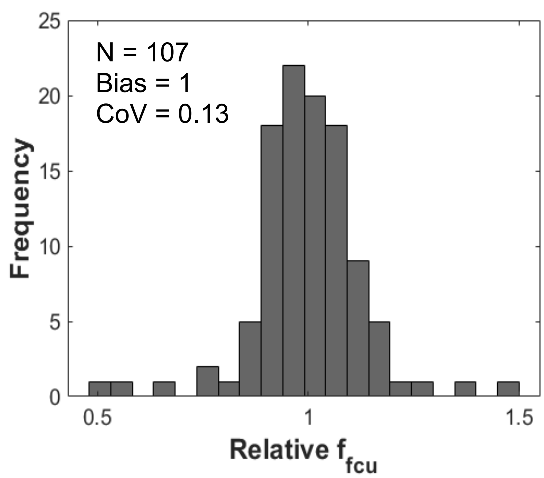

Figure 3: Distribution of GFRP bars in compression

3 PARAMETRIC STUDY

A parametric study was conducted to evaluate the reliability indexes corresponding to a select range of stability resistance factors. The considered sections had the following properties: 254 mm wide square sections, two layers of reinforcement, GFRP bar tensile and compression strength of 700 MPa and 560 MPa, respectively, GFRP bar modulus of elasticity of 45 GPa, reinforcement depth ratio of 0.8, and end moment ratio of 1. The parameters considered in the parametric study are summarized in Table 1.

The results of the parametric study are shown in Figure 4. The points in Figure 4 correspond to the average points obtained for each select case. The reliability index decreases with the increase in concrete strength, slenderness ratio, and eccentricity ratio as shown in Figure 4(a), Figure 4(c), and Figure 4(d), respectively. The reinforcement ratio was not considered as effective as the other studied parameters as shown in Figure 4(b).

As expected, the reliability index decreases with the increase in the eccentricity ratio and slenderness ratio since the latter magnifies the secondary moment effects. The decrease in column reliability as the concrete compressive strength increases may seem counterintuitive at first. This trend is explained as follows: higher concrete strength is associated with higher load mean values for a utilization ratio of 1.0 (ratio of factored loads to factored capacity). The higher loads applied on the section with high concrete strength cause the reliability of the section to drop as compared with counterpart sections having lower concrete strength.

Table 1: Parameters considered in the parametric study

Parameter	Value	No. of cases
concrete strength (f_c)	20, 40, 60	3
Reinforcement ratio (ρ)	1, 2, 4 %	3
Eccentricity ratio (e/h)	0.1, 0.3, 0.5, 1	4
Dead-to-live load ratio (D/L)	1, 2, 3, 4	4
Slenderness ratio (λ)	17, 22, 27, 33	4
Stability reduction factor (Φs)	0.65, 0.7, 0.75, 0.8, 0.85, 0.9	6
Total cases		6 x 576 3,456

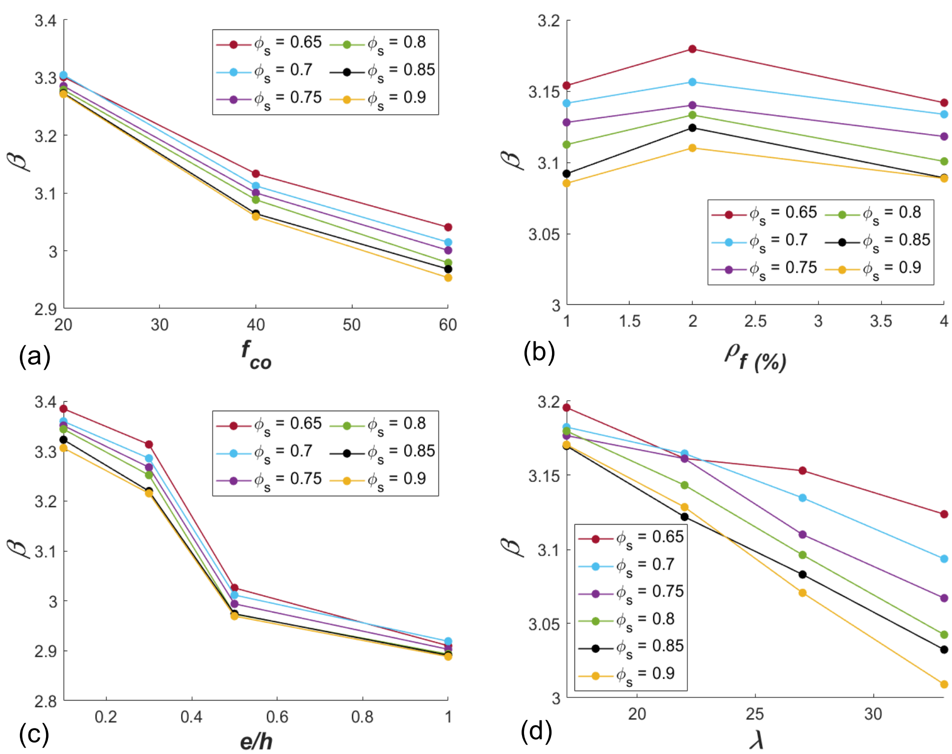

Figure 4: Effect of considered parameters on the reliability index, β: (a) effect of concrete strength, f_{co}; (b) effect of FRP reinforcement ratio, ρ_f (%); (c) effect of eccentricity ratio, e/h; and (d) effect of slenderness ratio, λ

4 RESULTS AND DISCUSSION

The reliability indexes for a select range of stability reduction factors, Φ_s, and dead-to-live load ratios, D/L, are shown in Table 2 and Figure 5. The results showed that a D/L ratio of 4 correlates to the worst-case loading scenario (Oudah et al. 2019). The stability reduction factors are equal to or greater than 3.0 which corresponds to the target reliability index set by Mirza et al. (1987) for calibrating the stiffness reduction factor for compression-controlled steel-reinforced concrete columns. It is concluded that the safety associated with the stiffness reduction factor of 0.75 for GFRP-RC columns proposed by ACI 440 aligns with the safety margin defined for steel-reinforced counterparts designed according to ACI 318-19 (2019) for the limited cases used in this study. Further research is needed to validate this conclusion for a wider range of input parameters and design cases.

Table 2: Reliability indexes for a select range of stiffness reduction factors and load ratios

D/L	Stiffness reduction factors, ϕ_s					
	0.65	0.7	0.75	0.8	0.85	0.9
1	3.30	3.28	3.26	3.26	3.25	3.25
2	3.18	3.17	3.15	3.13	3.13	3.11
3	3.09	3.09	3.08	3.06	3.03	3.03
4	3.06	3.04	3.02	3.01	3.00	2.99
Mean*	3.16	3.14	3.13	3.12	3.10	3.09
STD*	0.28	0.27	0.28	0.29	0.28	0.28
COV*(%)	8.88	8.73	8.88	9.16	9.02	9.06

* the mean was calculated based on all results.

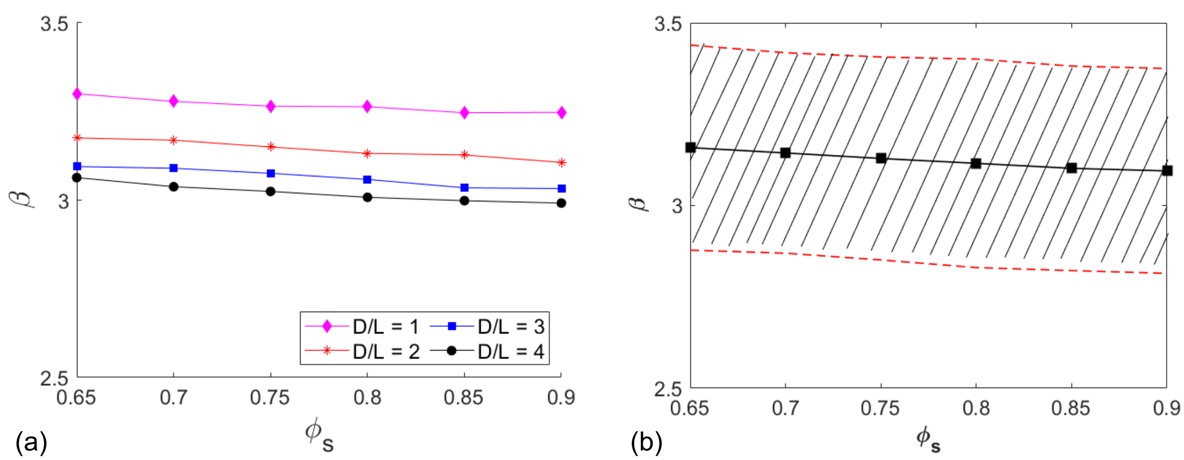

Figure 5: Reliability index, β, versus stiffness reduction factor, ϕ_s: (a) effect of dead-to-live ratios, *D*/*L*; and (b) average of all analyses plus and minus one standard deviation

5 CONCLUSION

The reliability indexes corresponding to a select range of stiffness reduction factors (0.65 to 0.9) used in the moment magnification method for the second-order analysis of GFRP-RC columns were quantified in this study. A parametric reliability-based analysis was conducted to quantify the reliability indexes. The parametric study considered 3,456 cases with various concrete strengths, dead-to-live load ratios, eccentricity ratios, slenderness ratios, and GFRP bar reinforcement ratios. Analysis results indicated a reliability index of 3.02 for a stability reduction factor of 0.75 (the value used in ACI 440) which approximately corresponds to the target reliability index used for calibrating the stiffness reduction factor in ACI318-19. The analysis results are preliminary. Further research is needed to validate the conclusions drawn from this study by considering a wider range of input parameters and design cases.

6 REFERENCES

ACI (American Concrete Institute). 2019. Building Requirements for Structural Concrete and Commentary. ACI 318-19, Farmington Hills, MI, USA.

ACI (American Concrete Institute). 1983. Building Requirements for Structural Concrete and Commentary. ACI 318-83, Farmington Hills, MI, USA.

AlAjarmeh, O. S., Manalo, A. C., Benmokrane, B., Vijay, P. V., Ferdous, W., and Mendis, P. 2019. Novel testing and characterization of GFRP bars in compression. *Construction and Building Materials*, **225**: 1112-1126.

CSA (Canadian Standards Association). 2019. Design of Concrete Structures. CSA A23.3-19, Rexdale, ON, Canada.

Hadhood, A., Mohamed, H. M., Benmokrane, B., Nanni, A., and Shield, C. K. 2019. Assessment of design guidelines of concrete columns reinforced with glass fiber-reinforced polymer bars. *ACI Structural Journal*, **116**(4): 193-207.

Khorramian, K. 2020. Short and Slender Concrete Columns Internally or Externally Reinforced with Longitudinal Fiber-Reinforced Polymer Composites. *Ph.D. Thesis*, Dalhousie University, Halifax, NS, Canada.

Khorramian, K., Oudah, F., and Sadeghian, P. 2021. Second-Order Analysis Of Slender GFRP Reinforced Concrete Columns using Artificial Neural Network. *CSCE Annual Conference 2021*, Online, STR180-1:STR180-9.

Khorramian, K., and Sadeghian, P. 2017a. Experimental and analytical behavior of short concrete columns reinforced with GFRP bars under eccentric loading. *Engineering structures*, **151**: 761-773.

Khorramian, K., and Sadeghian, P. 2017b. Short concrete columns reinforced with GFRP rebars under eccentric loading. *CSCE Annual Conference 2017*, Vancouver, BC, Canada, **532**-1:7.

Khorramian, K., and Sadeghian, P. 2018. New testing method of GFRP bars in compression. *CSCE Annual Conference 2018*, Fredericton, NB, Canada.

Khorramian, K., and Sadeghian, P. 2019. Material characterization of GFRP bars in compression using a new test method. *Journal of Testing and Evaluation*, **49**(2): 1037-1052.

Khorramian, K., and Sadeghian, P. 2020. Experimental Investigation of Short and Slender Rectangular Concrete Columns Reinforced with GFRP Bars under Eccentric Axial Loads. *Journal of Composites for Construction*, **24**(6): 04020072.

Mirza, S. A., Lee, P. M., and Morgan, D. L. 1987. ACI stability resistance factor for RC columns. *Journal of Structural Engineering*, **113**(9): 1963-1976.

Nowak, A. S., and Collins, K. R. 2012. *Reliability of structures*. 2nd ed., CRC press, Boca Raton, FL, USA.

Nowak, A. S., and Szerszen, M. M. 2003. Calibration of design code for buildings (ACI 318): Part 1-Statistical models for resistance. *ACI Structural Journal*, **100**(3): 377-382.

Oudah, F., El Naggar, M. H., and Norlander, G. 2019. Unified system reliability approach for single and group pile foundations–Theory and resistance factor calibration. *Computers and Geotechnics*, **108**: 173-182.

Shield, C. K., Galambos, T. V., and Gulbrandsen, P. 2011. On the history and reliability of the flexural strength of FRP reinforced concrete members in ACI 440.1 R. *ACI Special Publication*, **275**: 1-18.

Zadeh, H. J., and Nanni, A. 2017. Flexural Stiffness and Second-Order Effects in Fiber-Reinforced Polymer-Reinforced Concrete Frames. *ACI Structural Journal*, **114**(2): 193-207.